THE JOURNAL OF BIOLOGICAL CHEMISTRY Vol. 279, No. 47, Issue of November 19, pp. 48543–48549, 2004

Printed in U.S.A.

Origin of the 701-nm Fluorescence Emission of the Lhca2 Subunit of Higher Plant Photosystem I*

Received for publication, August 4, 2004, and in revised form, August 24, 2004
Published, JBC Papers in Press, August 24, 2004, DOI 10.1074/jbc.M408908200

Roberta Croce‡§, Tomas Morosinotto¶‖, Janne A. Ihalainen, Agnieszka Chojnicka**, Jacques Breton‡‡, Jan P. Dekker**, Rienk van Grondelle**, and Roberto Bassi¶‖**

*From the ‡Istituto di Biofisica, CNR, Trento, c/o ITC via Sommarive 18, Povo, Trento 38100, Italy, ¶Dipartimento Scientifico e Tecnologico, Università di Verona, 15 Strada Le Grazie, Verona 37134, Italy, ‖Université Aix-Marseille II, LGBP- Faculté des Sciences de Luminy, Département de Biologie, Case 901, 163 Avenue de Luminy, Marseille 13288, France, **Faculty of Science, Division of Physics and Astronomy, Vrije Universiteit, De Boelelaan 1081, 1081 HV Amsterdam, The Netherlands, and ‡‡Service de Bioenergetique, Bat. 532, Commissariat a l'Energie Atomique, Saclay, Gif-sur-Yvette Cedex 91191, France*

Photosystem I of higher plants is characterized by red-shifted spectral forms deriving from chlorophyll chromophores. Each of the four Lhca1 to -4 subunits exhibits a specific fluorescence emission spectrum, peaking at 688, 701, 725, and 733 nm, respectively. Recent analysis revealed the role of chlorophyll-chlorophyll interactions of the red forms in Lhca3 and Lhca4, whereas the basis for the fluorescence emission at 701 nm in Lhca2 is not yet clear. We report a detailed characterization of the Lhca2 subunit using molecular biology, biochemistry, and spectroscopy and show that the 701-nm emission form originates from a broad absorption band at 690 nm. Spectroscopy on recombinant mutant proteins assesses that this band represents the low energy form of an excitonic interaction involving two chlorophyll *a* molecules bound to sites A5 and B5, the same protein domains previously identified for Lhca3 and Lhca4. The resulting emission is, however, substantially shifted to higher energies. These results are discussed on the basis of the structural information that recently became available from x-ray crystallography (Ben Shem, A., Frolow, F., and Nelson, N. (2003) *Nature* 426, 630–635). We suggest that, within the Lhca subfamily, spectroscopic properties of chromophores are modulated by the strength of the excitonic coupling between the chromophores A5 and B5, thus yielding fluorescence emission spanning a large wavelength interval. It is concluded that the interchromophore distance rather than the transition energy of the individual chromophores or the orientation of transition vectors represents the critical factor in determining the excitonic coupling in Lhca pigment-protein complexes.

Photosystems I and II have a common general organization including a core complex moiety, binding Chl[1] *a* and β-carotene, and an outer antenna moiety, binding Chl *a*, Chl *b*, and xanthophylls. Nonetheless, their spectroscopic properties are substantially different. Both compartments of the PSI supercomplex are enriched in red-shifted chlorophyll absorption forms, whereas those of PSII are not. This property of PSI results in a preferential light harvesting in the near infrared spectral region (>700 nm) and causes the so-called "Emerson effect" that opened the way to the discovery of the two photosystems (1). In green plants, LHCI, the outer antenna of PSI, is the most red form-enriched compartment and is composed of four different complexes, the products of the genes *lhca1* to -4 (2). These complexes are located on one side of the core complex (3, 4) and can be isolated as dimers (5). The Lhca proteins belong to the Lhc multigenic family, and they share high sequence homology with the antenna complexes of PSII (6). Despite these strong similarities, the spectroscopic properties of Lhca and Lhcb complexes are very different. In particular, the emission spectrum of LHCI peaks at 733 nm, more than 50 nm red-shifted as compared with the emission spectra of the antenna system of PSII (LHCII) (7). *In vitro* reconstitution has shown that the red-shifted Chls are a common characteristic of Lhca complexes, although their energies differ strongly in different subunits. Emission forms at 701–702 nm have been found associated with Lhca1 and Lhca2, whereas 725- and 733-nm emissions were reported for Lhca3 and Lhca4, respectively (5, 8–11). It has been shown that the red emission of Lhca3 and Lhca4 originates from the low energy absorption band of an excitonic interaction involving Chl a in sites A5 and, probably, B5 (12), whereas the difference in energy is associated with the nature of the Chl A5 ligand, since the substitution of Asn in Lhca3 and Lhca4 by His, the usual ligand for Chl A5 in Lhc complexes, leads to the loss of the red spectral forms (12). In the present work, we analyze in detail Lhca2 with the aim of understanding the origin of the 701-nm emission that dominates the fluorescence spectrum at low temperature. It should be noticed that Lhca bears His as a ligand for Chl A5, yet its fluorescence emission is red-shifted by 20 nm with respect to the highly homologous subunit Lhcb6 (CP24) and other Lhcb proteins, thus opening the question of whether a different mechanism of modulation for the physico-chemical properties of chromophores is at work in Lhca2. By performing a detailed analysis by biochemical and spectroscopic methods on WT and mutant Lhca recombinant proteins, we conclude that the fluorescence emission band at 701 nm derives from excitonic coupling between chromophores A5 and B5, despite the presence of a His ligand for Chl A5. These results are discussed on the basis of the structural information that re-

* This work was supported by Ministero dell'Istruzione Universita'e Ricerca Progetti Fondo per gli Investimenti della Ricerca di Base Grants RBAU01E3CX and RBNE01LACT and by European Community Human Potential Program Grant HPRN-CT-2002-00248. The costs of publication of this article were defrayed in part by the payment of page charges. This article must therefore be hereby marked "*advertisement*" in accordance with 18 U.S.C. Section 1734 solely to indicate this fact.

§ To whom correspondence should be addressed. Tel.: 390461405360; Fax: 390461405372; E-mail: croce@itc.it.

[1] The abbreviations used are: Chl, chlorophyll; FWHM, full-width half-maximum; LD, linear dichroism; LHCI and LHCII, light-harvesting complex I and II, respectively; PSI and PSII, photosystem I and II, respectively; WT, wild type.

cently became available from x-ray crystallography (1, 13). We suggest that in green plant LHCI, differences in interchromophore distances rather than in transition energies of the individual chromophores of the interacting pair or in the orientation of their transition vectors represent the critical factor in determining excitonic coupling.

EXPERIMENTAL PROCEDURES

DNA Constructions and Isolation of Overexpressed Lhca Apoproteins from Bacteria—cDNAs of Lhca2 from *Arabidopsis thaliana* (11) were mutated with the QuikChange® site-directed mutagenesis kit, by Stratagene. WT and mutant apoproteins were isolated from the BL21 strain of *Escherichia coli* transformed with these constructs following a protocol previously described (14, 15).

Reconstitution and Purification of Protein-Pigment Complexes—Reconstitution and purification were performed as described in Ref. 16 with the following modifications. The reconstitution mixture contained 420 μg of apoprotein, 240 μg of chlorophylls, and 60 μg of carotenoids in a total of 1.1 ml. The Chl *a*/*b* ratio of the pigment mixture was 4.0. The pigments used were purified from spinach thylakoids.

Protein and Pigment Concentration—High pressure liquid chromatography analysis was as in Ref. 17. The chlorophyll to carotenoid ratio and Chl *a*/*b* ratios were independently measured by fitting the spectrum of acetone extracts with the spectra of individual purified pigments in 80% acetone (18).

Spectroscopy—The absorption spectra at room temperature and 77 K were recorded using an SLM-Aminco DK2000 spectrophotometer, in 10 mM Hepes, pH 7.5, 20% glycerol (60% at low temperature) and 0.06% β-dodecylglucomaltoside. Wavelength sampling step was 0.4 nm, scan rate was 100 nm/min, and optical path length was 1 cm.

The absorption spectra at 4 K were measured using a home-built spectrophotometer at OD 0.5 in the same buffer as described above, but with 67% glycerol.

Fluorescence emission spectra at 77 K were measured using a Jasco FP-777 spectrofluorimeter and corrected for the instrumental response. The samples were excited at 440, 475, and 500 nm. The spectral bandwidth was 5 nm (excitation) and 3 nm (emission). The chlorophyll concentration was about 0.02 μg/ml in 60% glycerol and 0.03% β-dodecylglucomaltoside. The spectra between 130 and 4 K of the WT were measured with a 0.5-m imaging spectrograph (Chromex 500IS) and a CCD camera (Chromex Chromcam I). For broad band excitation, a tungsten halogen lamp (Oriel) was used with band pass filters transmitting at 420, 475, and 506 nm. For narrow band excitation, a dye laser (Coherent CR599) was used, which was pumped by an argon ion laser (Coherent Inova 310). The optical bandwidth of the laser was 0.6 nm, and the power was kept at 0.15 milliwatts/cm^2. The spectra were corrected for the wavelength dependence of the detection system.

CD spectra were measured at 10 °C on a Jasco 600 spectropolarimeter. The wavelength sampling step was 0.5 nm, the scan rate 100 nm/min, and spectra were recorded with eight accumulations. The OD of the samples was 1 at the maximum in the Qy transition for all complexes, and the samples were in the same solution as described for the absorption measurements. All spectra presented were normalized to the polypeptide concentration based on the Chl binding stoichiometry.

LD spectra were measured as described in Ref. 19 using samples oriented by the polyacrylamide gel squeezing technique.

RESULTS

Analysis of Lhca2-WT Complex—Lhca2 WT was obtained by overexpression of the apoprotein in *E. coli* and reconstitution *in vitro* with pigments. The complex was purified from excess pigment and unfolded apoprotein by sucrose gradient ultracentrifugation, anion exchange chromatography, and glycerol gradient ultracentrifugation and was obtained in monomeric form, as previously described (11).

Absorption—The absorption spectrum of Lhca2 at 4 K shows its maximum in the Chl Qy region at 679.5 nm, whereas in the Chl *b* region two local maxima can be detected at 644 and 652 nm (Fig. 1). The second derivative analysis allows resolution of several absorption forms: three Chl *b* at 643, 651, and 653 nm and four Chl *a* at 661, 672, 680.5, and 688.5 nm. In the blue region, the minimum at 497 nm is associated to the redmost peak ($S_0 > S_{2,0}$ transition) of the carotenoids, whereas those at 480 and 471 nm may represent the Soret bands of two Chl *b* spectral forms.

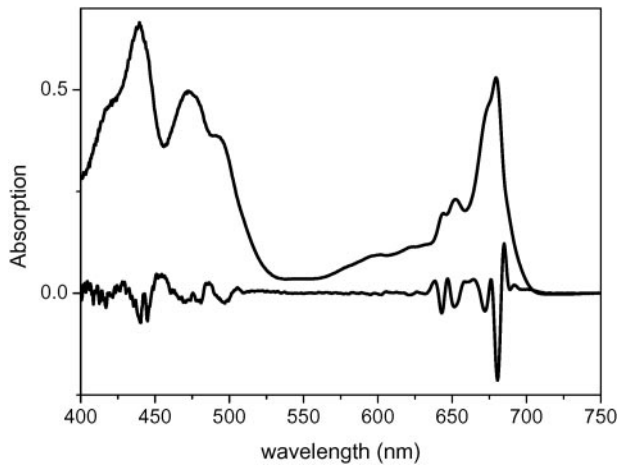

FIG. 1. **Absorption spectrum at 4 K of Lhca2-WT.** The spectrum is presented together with its second derivative.

Fluorescence Measurements—Fluorescence emission spectra of Lhca2 were measured at different temperatures upon excitation in the blue spectral region (Fig. 2). Two emission forms at 688 and 701 nm can be detected. The latter dominates the spectrum at 4 K, but the 688-nm form is still present, indicating that the energy transfer between these two forms is not complete, thus suggesting some kind of heterogeneity in the sample.

In order to obtain information on the origin of the two fluorescence emissions, fluorescence emission spectra upon selective excitation in the Qy band of the complex were measured. A selection of spectra is presented in Fig. 3*A*. The relative contribution of the 688- and 701-nm forms changed as a function of the excitation wavelength. In particular, the 688-nm emission reached its maximum for excitations in the 680–683-nm range, indicating that it originates from the red part of the bulk absorption. For excitation above 685 nm, the amplitude of the 688-nm emission band drops considerably, and the spectrum is dominated by the low energy emission form.

In Fig. 3*B*, the excitation wavelength is plotted *versus* the maximum of the emission (squares). By increasing the excitation wavelength from 680 to 685 nm, a blue shift of the emission maximum of the redmost form to 697 nm (excitation at 685 nm) is observed. This blue shift is due to the contribution to the emission of a larger fraction of "red" pigments absorbing in the blue wing of the inhomogeneous distribution, which are selectively excited at this wavelength (20, 21). Above 685 nm, the emission maximum undergoes a red shift, exhibiting a linear relation with the excitation wavelength, thus reaching a value of 701 nm for excitation at 690 nm. By exciting in the redmost part of the absorption spectrum, a further red shift of the emission maximum was observed. For excitations within the red tail of the absorption spectrum (around 710 nm), the emission maximum is still broad (340 cm^{-1}), indicating large homogeneous broadening. Moreover, for excitation above 700 nm, site selection does not have a strong influence on the shape and the width of the emission, thus suggesting that the spectrum is dominated by inhomogeneous broadening.

The site-selected fluorescence data allow also determining the peak wavelength of the absorption form responsible for the 701-nm emission. This value corresponds to the excitation wavelength at which the emission peak coincides with that in spectra obtained from nonselective excitation (see Ref. 20 for more details). By following this procedure, the absorption maximum of the red band is calculated to be approximately at 690 nm, in agreement with the second derivative analysis of the

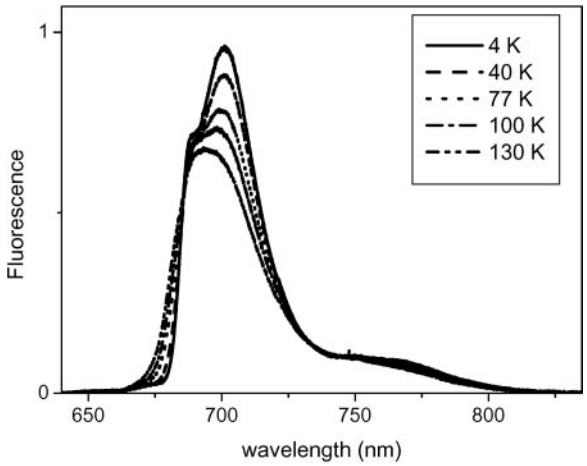

FIG. 2. **Temperature dependence of the fluorescence emission spectrum.** Fluorescence emission spectra of Lhca2-WT measured at 4, 40, 77, 100, and 130 K. The sample was excited at 506 nm.

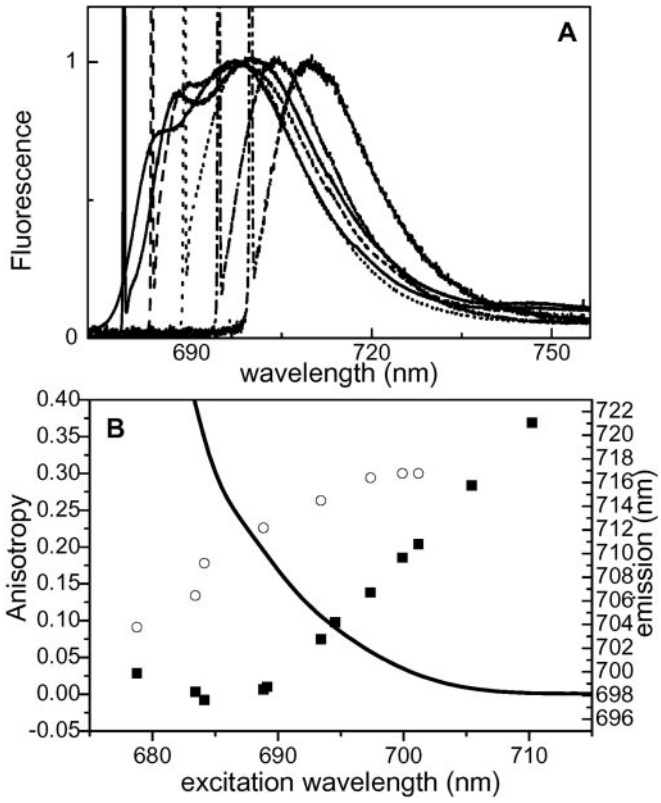

FIG. 3. **Site-selected fluorescence.** *A*, selection of emission spectra of Lhca2 at 4 K, laser excitation at 679, 683, 689, 694, and 700 nm. The spectra were normalized to the maximum of the emission. The sharp peak is largely due to elastic scattering of the laser excitation light. *B*, emission and absorption characteristics of Lhca2-WT complex at 4 K. *Closed squares*, dependence of the emission maximum as a function of the excitation wavelength. *Open circles*, value of the anisotropy of the emission detected at 701 nm. *Line*, tail of the absorption spectrum.

absorption spectrum, which showed the redmost absorption form at 688.5 nm (see Fig. 1).

Additional information on the characteristics of the red absorption tail can be obtained by fluorescence anisotropy measurements, which gives an indication of the orientation of the absorbing and emitting dipoles. In Fig. 3*B* (*circles*), the values of the fluorescence anisotropy detected at 701 nm are reported as a function of the excitation wavelength. It is clear that the values of the anisotropy also depend on the excitation wavelength. Upon excitation around 680 nm, the anisotropy value is

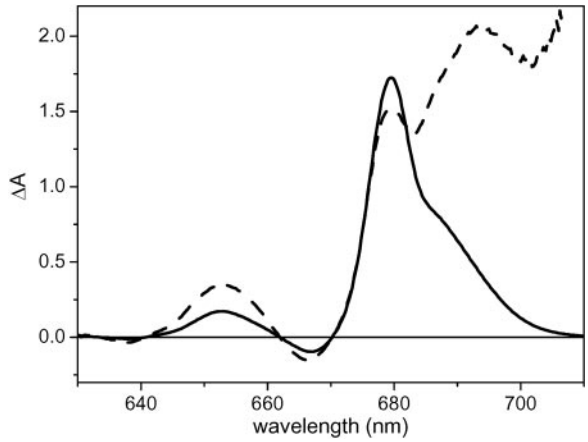

FIG. 4. **Linear dichroism.** LD (*solid line*) and LD/3OD (*dashed line*) spectra of Lhca2-WT at 10 K. The scale is in arbitrary units.

low, and it rises to a maximum of 0.32 for excitation wavelength above 697 nm, a value very similar to that obtained in the analysis of the 702-nm emission form in a native LHCI preparation (7). This result indicates that above this wavelength, no depolarization due to energy transfer takes place, thus suggesting that the same band is responsible for the absorption and the emission. The alternative hypothesis of energy transfer between pigments having the same dipole transition orientation is extremely unlikely.

LD Spectra—The LD spectrum of Lhca2 shows strong positive contribution in the Chl *a* Qy absorption region, with a maximum at 679.5 nm and a shoulder around 690 nm (Fig. 4). The signal becomes slightly negative at 667 nm. In the Chl *b* absorption region, a positive contribution is observed at 653 nm. The reduced LD spectrum (*LD/3A*) shows the largest value around 690 nm, indicating that the Chl(s) responsible for this absorption forms is oriented with the largest angle with respect to the normal to the membrane plane. A second positive LD value corresponds to the maximum of the absorption spectrum (679.4 nm), whereas a local minimum is present at 683 nm.

Localization of the Low Energy Absorbing Form(s) into the Lhca2 Structure—The above measurements strongly indicate that the red-shifted fluorescence signal at 701 nm is associated with an absorption form peaking at 690 nm. In order to identify which chromophore is responsible for this absorption, mutation analysis at selected Chl-binding residues was performed. Based on previous analysis with Lhca3 and Lhca4 (12), residues coordinating Chl A5, B5, and B6, involved in the low energy absorption forms, were mutated to nonbinding residues (*i.e.* which cannot coordinate the central magnesium of the Chls) (see Table I for details). The apoprotein was expressed in *E. coli*, and the complex was reconstituted *in vitro* with pigments. In all cases, stable monomeric complexes were obtained. The pigment content of the complexes is shown in Table I.

The decreased Chl/Car ratio observed in all mutants indicates loss of Chls in the Chl binding site mutants, and the higher Chl *a*/*b* ratio as compared with the WT complex implies that Chl *b* molecules are preferentially lost. Normalization to the carotenoid content would indicate loss of one Chl in the A5 mutant, two Chls in B5, and one Chl in B6. However, this stoichiometry may not be correct in the case of mutants A5 and B5, since the corresponding mutants in all other Lhca complexes showed a loss of carotenoid molecules. Moreover, loss of one Chl in A5 would indicate that this site has mixed occupancy, which is very unlikely, because the A5 site has been found to accommodate one Chl a molecule in all complexes analyzed so far (22–24). We thus suggest that the A5 mutant loses two Chls molecules, one Chl *a* and one Chl *b*, as was the

TABLE I
Pigment composition of the complexes
The amount of caroteonids is calculated for the given Chl stoichiometry. The error in the data is less than 0.1.

Sample	Mutation	Chl *a/b*	Chl/Caroteonid	Chl total	Lutein	Violaxanthin
RLhca2-WT		2.1	5.0	10	1.68	0.32
RLhca2-A5	H52F	2.2	4.5	8	1.41	0.35
RLhca2-B5	E108V/R111L	4.7	4	7	1.44	0.3
RLhca2-B6	E100V	3.1	4.4	9	1.57	0.25

case in Lhca1, whereas a small loss of carotenoids accounts for the change in Chl/Car ratio. The B5 mutant loses most probably three Chl molecules, two Chls *b* and one Chl *a*. The loss of Chl *a* is consistent with the analysis of the absorption spectrum (see below), which is strongly affected in the Chl *a* Qy absorption region.

To check the influence of the mutation on the 701-nm emission form of the complex, fluorescence emission spectra at 77 K were measured (Fig. 5). Mutant A5 and B5 showed emission maximum at 686 nm, thus shifted by 15 nm to the blue as compared with the WT peak, indicating that both mutations affect the low energy emission form. The fluorescence emission of the B6 mutant was, instead, very similar to that of the WT, showing that mutation at this Chl binding site does not influence the chromophore(s) responsible for the 701-nm emission.

The absorption spectra of the three mutants and the WT at 77 K are presented in Fig. 6*A* and the second derivative of the spectra are shown in Fig. 6*B*.

Mutant A5 was mainly affected in the Chl *a* region, where the absorption form at 690 nm disappeared. A decrease in the amplitude of the spectrum in the Chl *b* region could also be observed, in agreement with the Chl *b* loss (see Table I). Mutant B5 showed dramatic changes in the absorption spectrum as compared with the WT; not only two Chl *b* forms (at 642 any 651 nm) were lost, but also a 688-nm absorbing Chl *a* form. Absorption at 680 nm was also decreased and was partially compensated by the increased signal at 670 nm, possibly due to the presence of unconnected Chls. Mutant B6 was affected mainly in the Chl *b* region, where the absorption at 642 nm disappeared, an indication that the Chl *b* accommodated in the B6 site absorbs at this wavelength. Minor changes could also be detected in the Chl *a* absorption region. Interestingly, the effect of the mutation at site B6 on the red-shifted absorption forms is different in Lhca2 as compared with Lhca1 (24) and Lhca4.[2] In these homologous proteins, loss of Chl B6 significantly affected the red-shifted emission forms. This difference may be related to the observation that the B6 mutants of Lhca1 and Lhca4 lose xanthophylls, whereas Lhca2 did not. The loss of red forms in Lhca1 and Lhca4 upon mutation at site B6 was interpreted as an indirect effect mediated by the carotenoid molecule (24). The different results obtained for the B6 mutant in Lhca2 seem to indicate that the carotenoid organization in the Lhca complexes is different with respect to others Lhca subunits.

The CD spectra at room temperature of WT and mutants are reported in Fig. 7. Mutant A5 is identical in the Chl *b* region to the WT but shows strong differences in the Chl *a* region. Comparison with the WT spectrum indicates that this mutant loses a negative CD signal at 687 nm and a positive one at 672 nm, thus suggesting loss of an excitonic interaction. A strong decrease in the intensity of the CD signal in the Chl *b* region is observed for both B6 and B5 mutants, thus implying that the Chl *b* molecules lost in the B5 and B6 mutants participate in pigment-pigment interactions. In particular, the comparison of the spectra of the WT with the one of mutant B6 shows that, in

[2] T. Morosinotto, R. Bassi, and R. Croce unpublished results.

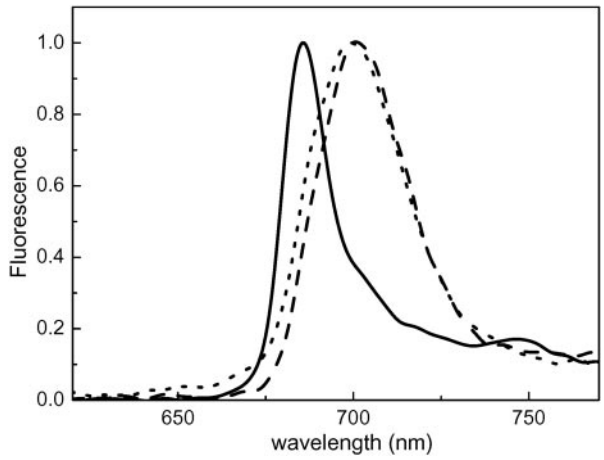

FIG. 5. **Fluorescence emission spectra at 77 K of Lhca2 WT and mutants Lhca2-WT (*dashed line*), Lhca2-A5 mutant (*solid line*), and Lhca2-B6 mutant (*dotted line*) upon excitation at 500 nm.** The spectra were normalized to the maximum of the emission.

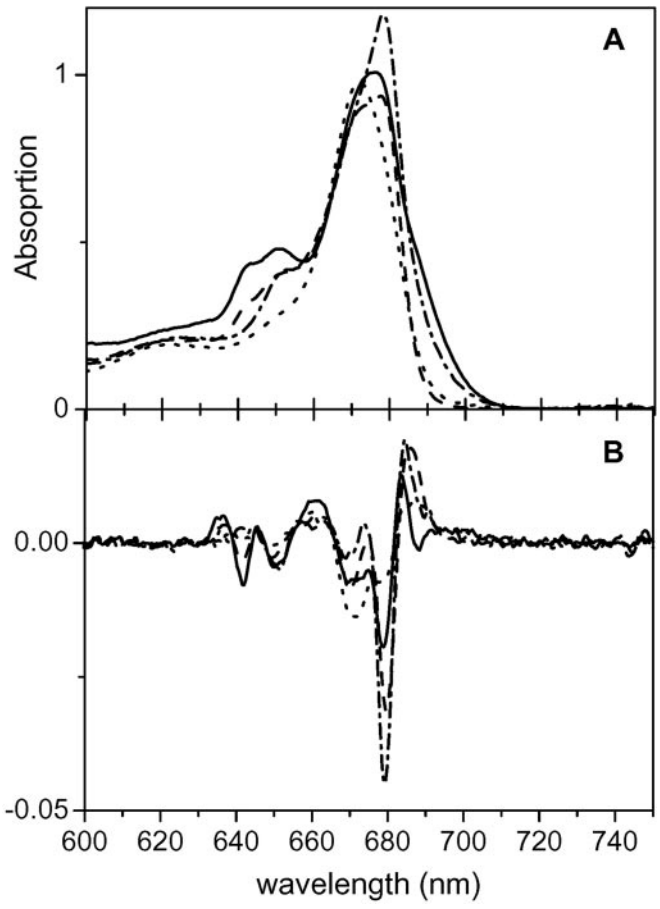

FIG. 6. **Absorption spectra at 77 K of Lhca2-WT and mutants.** *A*, absorption spectra of Lhca2-WT (*solid line*), Lhca2-A5 (*dashed line*), Lhca2-B5 (*dotted line*), and Lhca2-B6 (*dashed and dotted line*). The spectra are normalized to the Chl content. *B*, second derivative of the spectra reported in *A*.

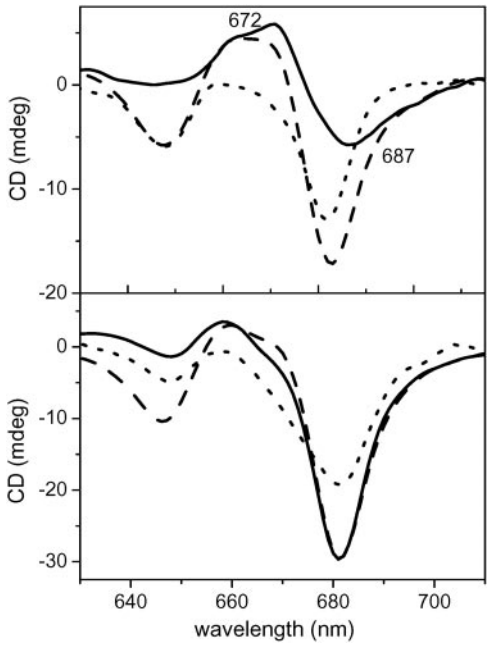

FIG. 7. **Circular dichroism spectra of Lhca2-WT and mutants at 10 °C.** All of the spectra are normalized to the absorption (*A*): Lhca2-WT (*dashed line*), Lhca2-A5 (*dotted line*), and difference WT-A5 (*solid line*). *B*, Lhca2-WT (*dashed line*), Lhca2-B5 (*dotted line*), Lhca2-B6 (*solid line*).

the latter, the loss of the negative signal in the Chl *b* region is connected with the loss of a positive contribution in the Chl *a* region (around 670 nm), thus suggesting the presence of a Chl *b*-Chl *a* interaction.

DISCUSSION

The current results show that Lhca2 takes a unique position within the LHCI proteins. Unlike Lhca3 and Lhca4, it does not show strong absorption above 700 nm, but nevertheless its emission is still 22-nm red-shifted as compared with the emission maxima of all Lhcb complexes. In the case of Lhca3 and Lhca4, it was shown that the red absorption is associated with the presence of an Asn as ligand for Chl A5 (12). This is not the case of Lhca2, which has a His in this position, a feature shared with all Lhcb proteins that do not show red-shifted Chl forms. We thus proceeded with the analysis of the chromophore organization in Lhca2 and identified the absorption band responsible for the 701-nm emission band, with the aim of understanding the mechanism that allows modulation of the physicochemical properties of chlorophyll ligands.

Lhca2 has been shown to have the emission maximum at 701 nm (at 4 K). A second emission form was also detected at 688 nm in the 4 K spectrum, thus suggesting heterogeneity in the sample. Several sources of spectroscopic heterogeneity have been reported for Lhc proteins, including phosphorylation-induced spectral changes in CP29 (25), the presence of multiple gene products in the LHCII preparations with different spectral features (26), and conformational changes induced by zeaxanthin binding to site L2 (27, 28). In the present work, a recombinant Lhca2 preparation was analyzed, which was the product of a single gene, did not contain zeaxanthin, was monomeric as detected by sucrose gradient ultracentrifugation, and was not phosphorylated. We conclude that the persistence of the two fluorescence emission bands is the product of a previously unrecognized source of molecular heterogeneity, which is reflected in the establishment or not of the molecular feature responsible for the 701-nm emission. Two hypotheses can be proposed for explanation of these data; either the Lhca2 protein is present into two conformations in which the two interacting chromophores are set at different distances and/or different orientations with respect to each other, or one of the two sites can be occupied by either Chl *a* or Chl *b*. The difference in transition energies between Chl *a* and Chl *b* and the difference in the orientation of the transition vectors (29) would make the observable spectral shift of a Chl *a*/Chl *b* interaction much smaller with respect to that of a Chl *a*/Chl *a* interaction. The likelihood of these hypotheses will be discussed below.

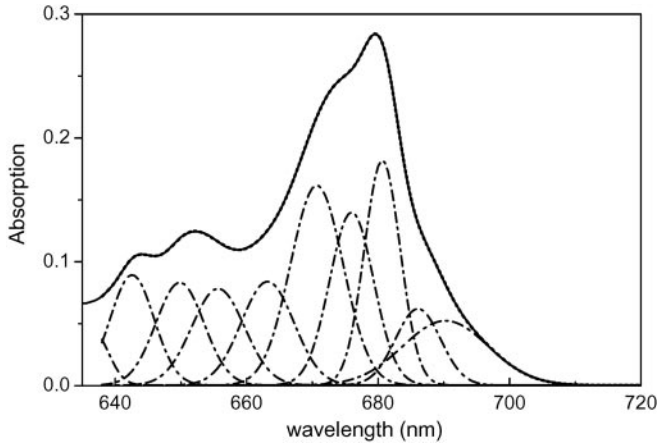

FIG. 8. **Gaussian description of the absorption spectrum of Lhca2-WT at 4 K.** 10 Gaussians are used to describe the spectrum.

Site-selected fluorescence measurements indicate that the 689-nm emission originates from bulk Chls absorbing around 682 nm, whereas the 701-nm emission form is associated with a Chl absorption form at 690 nm. This result is confirmed by the mutation analysis, which showed that both mutants losing the 701-nm emission also lack the 690-nm absorption form.

Spectral Characteristics of the 690-nm Absorption Form—In order to get more details on the 690-nm absorption form of Lhca2, the absorption spectrum of the WT complex was described in terms of Gaussian forms, using the values obtained by second derivative analysis as starting parameters (Fig. 8). Three Chl *b* bands were needed to describe the region between 640 and 660 nm, namely at 642, 649, and 655 nm. The red part of the Qy Chl *a* absorption region was described with two Gaussians at 686 and 690 nm, with the latter showing a broadened spectrum. An oscillation strength corresponding to the absorption of 0.85 Chl *a* molecules is associated with this band.

This description is in good agreement with the fluorescence data; the redmost band, which is responsible for the 701-nm emission, absorbs at 690 nm, as suggested by the site-selected fluorescence measurements, and a second band, peaking at 686 nm, is needed for description of the red absorption tail. The absorption of this second band fades to zero at around 697 nm, in agreement with the anisotropy measurements, which suggest that only above 697 nm, excitation energy is exclusively absorbed by the redmost pigment, whereas the 686-nm band is less broadened (8-nm FWHM), thus suggesting that this absorption derives from a monomeric pigment.

The energetic separation between the absorption maximum and the emission peak represents the Stokes shift. For the 690-nm absorption form, which emits at 701 nm, the Stokes shift is 11 nm (240 cm^{-1}). This is larger than observed in Lhcb complexes (where it is around 2 nm). From the Stokes shift, a value of the optical reorganization energy ($S\nu$) can be obtained, which corresponds to 120 cm^{-1} (Stokes shift $\simeq 2S\nu$.).

The characteristics of the absorption band broadening can yield important information on the chromophore protein environment. The analysis of the WT minus mutant difference spectra indicates that at 77 K the FWHM of the band is around

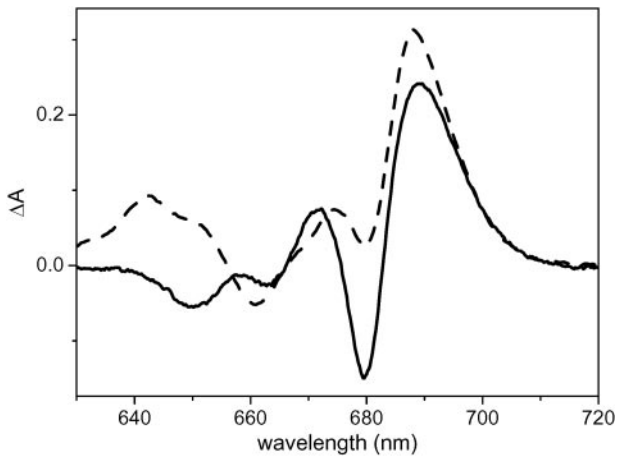

FIG. 9. **Comparison of the absorption (*dashed line*) and linear dichroism (*solid line*) difference spectra of WT and A5 mutants.**

400 cm^{-1}. At this temperature, the homogeneous broadening of the band can be described as follows,

$$FWHM^2_{hom} = 7.7 S\nu T \text{ with } FWHM^2 = FWHM^2_{hom} + FWHM^2_{ihn} \quad \text{(Eq. 1)}$$

where $FWHM^2 = FWHM^2_{hom} + FWHM^2_{ihn}$. Using the value of $S\nu$ obtained from the Stokes shift, the value for the $FWHM_{hom}$ is 270 cm^{-1}, which gives a value of the inhomogeneous broadening of around 300 cm^{-1}. Such a large value for the inhomogeneous broadening is consistent with data from site-selected fluorescence measurements, since the excitation in the red tail did not affect the shape and width of the emission band.

The 690-nm absorption form of Lhca2 is thus characterized by a larger value of both homogeneous and inhomogeneous broadening as compared with the bulk Chl absorption form, for which these two values are both around 100 cm^{-1} (30). In this respect, the 690-nm band of Lhca2 shows characteristics very similar to the red absorption forms observed in several organisms (20), although its energy is significantly higher.

The Origin of the 701-nm Emission—Large values of optical reorganization energy are usually associated with the presence of pigment-pigment interactions. It has already been suggested that the red forms of Lhca3 and Lhca4 are the low energy term of an interaction between two Chl *a* molecules. Mutational analysis shows that these two chromophores are bound to sites Chl A5 and Chl B5, since mutation at these sites completely abolishes the red emission forms. This conclusion is in agreement with the finding that site A5 binds Chl *a* in Lhca as well as in any other Lhc protein (22–24), whereas site B5 either binds Chl *a* or has a mixed Chl *a*-Chl *b* occupancy as derived from pigment analysis of WT and mutant protein as well as their spectroscopic analysis. We conclude that the low energy spectral forms originate from the same protein domain in all Lhca complexes and involve Chls A5 and B5. Nevertheless, the energy level of these red-shifted transitions is modulated to a different extent in each Lhca subunit.

The presence of pigment-pigment interaction inducing the absorption at 688–690 nm of Lhca2 is supported by the comparison of the CD spectra of WT and A5 mutant, which lack a negative contribution around 687 nm and a positive one at 672 nm (values at room temperature). Similar components can be detected in the WT minus A5 absorption and LD difference spectra (Fig. 9). In both cases, two absorptions, at 688–689 nm and at 672–674 nm, can be detected, representing Chl forms lost by the effect of the mutation at site A5 and having positive LD spectra. These data can be interpreted as the loss of an excitonic interaction having the low energy band at 688–690 nm and the high energy band at 672–674 nm, as the effect of A5 mutation. To describe both difference spectra, a negative band peaking at 679 nm is required. This band is present in the mutant but not in the WT and shows a positive LD signal (Fig. 6). Considering that all spectroscopic techniques consistently indicate that the interaction leading to the 690-nm absorption involves two Chl *a* molecules and that in the A5 mutant only one Chl *a* molecule is lost, the gain in the absorption can be interpreted as the contribution of the noninteracting monomer, which is left alone in the A5 mutant. Based on the mutation analysis, which suggested that the two interacting Chls are accommodated in sites A5 and B5, we conclude that the "new" 679-nm form detected in WT minus A5 difference spectra represents the absorption of the monomeric Chl *a* in site B5. This is in agreement with the analysis of the homologous protein CP29 (22), showing that a noninteracting Chl *a* absorbing at 679 nm is bound to site B5.

From the energetic distance between the two bands in the CD spectrum and considering the two monomers as isoenergetic, a value of 150 cm^{-1} for the interaction energy can be calculated (notice that a very similar value is obtained considering the absorption of monomeric A5 at 675 nm as was the case in all Lhc complexes analyzed so far (22, 23)). This value is half of the value observed for the interaction energy in Lhca3 and Lhca4.[3]

Once it is concluded that in all Lhca complexes the red forms originate from interaction between Chls *a* in sites A5 and B5, it is interesting to investigate the origin of the large difference in interaction energy between the complexes, which is reflected in a difference of around 30 nm between the emission maxima of Lhca2 and Lhca4. Two major factors control the amplitude of the interaction energy: the distance between the chromophores and the relative orientation of their dipole moment transition (the geometric factor k). ($V_{1,2} = 5.5k\mu_1\mu_2/R^3$, where R is the center to center distance between the chromophores and μ represents the dipole moment of the Chls). The analysis of the LD spectra of the complexes indicates that the redmost absorption form of both Lhca4 and Lhca2 forms the largest angle with the normal to the membrane plane (12) (this work). Although small differences in the orientation between the Chls in the two complexes cannot be excluded, we can assume, in a first approximation, a similar geometric factor in the two complexes. On this basis, the difference in interaction energy can be explained by considering that the distance between the two interacting Chls is around 2 Å larger in Lhca2 compared with Lhca4 by applying the equation, $V = 90k/R^3$. Recently, the structure of the PSI·LHCI complex has been elucidated at 4.4-Å resolution, and the position of the bound Chl has been defined. The center to center distance between Chl A5 and B5 in Lhca4 has been shown to be 7.9 Å, whereas in Lhca2 the value is 10.4 Å (3). This is consistent with the proposal that in Lhca4, the presence of the Asn as a ligand for Chl A5 allows a shorter distance between the two interacting Chls as compared with the complexes that have His for Chl A5 ligation (12).

Comparison with LHCII—Previous work with Lhca3 and Lhca4 has highlighted the importance of the presence of an Asn as ligand for Chl A5 for the generation of the red-shifted 730-nm fluorescence in Lhca3 and Lhca4, the only members of the Lhc superfamily holding Asn as a Chl A5 ligand. The present work shows that a significant, although lower, level of excitonic interaction can be obtained without the intervention of Asn ligation, and yet this interaction is sufficient for yielding the 701-nm emission form of Lhca2. This finding implies that additional structural signatures differentiate the Lhca from

[3] R. Croce, T. Morosinotto, J. A. Ihalainen, A. Chojnicka, J. P. Dekker, R. van Grondelle, and R. Bassi, manuscript in preparation.

the Lhcb subfamily as a requirement for the chromophore-chromophore interactions in the helix C domain. This problem can be addressed thanks to the recent elucidation of LHCII structure at high resolution, since in Lhcb 1–3, the components of trimeric LHCII, the ligand of Chl A5 is His, as in Lhca2, and yet no 701-nm fluorescence emission can be detected. Moreover, the two structures in this domain are also very similar (3, 13), thus allowing detailed comparison. Why does LHCII not have red forms? Both x-ray structure (13) and mutation analysis (23, 31) consistently identify the ligand at site B5 as Chl *b*. Although the distance and mutual orientation between Chl *a* A5 and Chl *b* B5 allow for interaction in LHCII (13), the large energy gap between Chl *a* and Chl *b* makes the shift induced in the absorption form very small. In the case of Lhca2, biochemical and spectral analysis are consistent with site B5 having low selectivity and thus allowing for binding of both Chl *a* and Chl *b*. This mixed occupancy is crucial to explain the presence of two emission forms in the emission spectrum of Lhca2. We suggest that the blue form (emission at 689 nm) originates from the population of the ensemble having Chl *b* in site B5, whereas the 701-nm emission is originating from the population in which site B5 accommodates a Chl *a* molecule. The crucial question is thus how the selectivity of each Chl binding site is determined in Lhca proteins. The structure of LHCII shows that all but one Chl *b* present have the formyl group hydrogen-bonded with protein residues of water molecules. It can thus be speculated that the possibility to form this hydrogen bond affects the affinity of a site for Chl *b* *versus* Chl *a*, through an energy minimization effect. In LHCII, Chl *b* in site B5 is stabilized by hydrogen bond with the NH of Gln^{131} (13). In the Lhca2 complex, as well as in all Lhca complexes, this Gln is substituted by a Glu residue. The Glu cannot act as hydrogen donor, and it can be expected that in this case Chl B5 loses its high affinity for Chl *b* and thus can also accommodate Chl *a*.

REFERENCES

1. Evans, J. R. (1986) *Photobiochem. Photobiophys.* **10,** 135–147
2. Haworth, P., Watson, J. L., and Arntzen, C. J. (1983) *Biochim. Biophys. Acta* **724,** 151–158
3. Ben Shem, A., Frolow, F., and Nelson, N. (2003) *Nature* **426,** 630–635
4. Boekema, E. J., Jensen, P. E., Schlodder, E., van Breemen, J. F., van Roon, H., Scheller, H. V., and Dekker, J. P. (2001) *Biochemistry* **40,** 1029–1036
5. Croce, R., Morosinotto, T., Castelletti, S., Breton, J., and Bassi, R. (2002) *Biochim. Biophys. Acta* **1556,** 29–40
6. Jansson, S. (1994) *Biochim. Biophys. Acta* **1184,** 1–19
7. Ihalainen, J. A., Gobets, B., Sznee, K., Brazzoli, M., Croce, R., Bassi, R., van Grondelle, R., Korppi-Tommola, J. E. I., and Dekker, J. P. (2000) *Biochemistry* **39,** 8625–8631
8. Schmid, V. H. R., Cammarata, K. V., Bruns, B. U., and Schmidt, G. W. (1997) *Proc. Natl. Acad. Sci. U. S. A.* **94,** 7667–7672
9. Zhang, H., Goodman, H. M., and Jansson, S. (1997) *Plant Physiol.* **115,** 1525–1531
10. Schmid, V. H. R., Potthast, S., Wiener, M., Bergauer, V., Paulsen, H., and Storf, S. (2002) *J. Biol. Chem.* **277,** 37307–37314
11. Castelletti, S., Morosinotto, T., Robert, B., Caffarri, S., Bassi, R., and Croce, R. (2003) *Biochemistry* **42,** 4226–4234
12. Morosinotto, T., Breton, J., Bassi, R., and Croce, R. (2003) *J. Biol. Chem.* **278,** 49223–49229
13. Liu, Z., Yan, H., Wang, K., Kuang, T., Zhang, J., Gui, L., An, X., and Chang, W. (2004) *Nature* **428,** 287–292
14. Nagai, K., and Thøgersen, H. C. (1987) *Methods Enzymol.* **153,** 461–481
15. Paulsen, H., Finkenzeller, B., and Kuhlein, N. (1993) *Eur. J. Biochem.* **215,** 809–816
16. Giuffra, E., Cugini, D., Croce, R., and Bassi, R. (1996) *Eur. J. Biochem.* **238,** 112–120
17. Gilmore, A. M., and Yamamoto, H. Y. (1991) *Plant Physiol.* **96,** 635–643
18. Croce, R., Canino, G., Ros, F., and Bassi, R. (2002) *Biochemistry* **41,** 7343
19. Haworth, P., Tapie, P., Arntzen, C. J., and Breton, J. (1982) *Biochim. Biophys. Acta* **682,** 152–159
20. Gobets, B., Van Amerongen, H., Monshouwer, R., Kruip, J., Rögner, M., van Grondelle, R., and Dekker, J. P. (1994) *Biochim. Biophys. Acta* **1188,** 75–85
21. den Hartog, F. T. H., Dekker, J. P., van Grondelle, R., and Völker, S. (1998) *J. Phys. Chem. B* **102,** 11007–11016
22. Bassi, R., Croce, R., Cugini, D., and Sandona, D. (1999) *Proc. Natl. Acad. Sci. U. S. A.* **96,** 10056–10061
23. Remelli, R., Varotto, C., Sandona, D., Croce, R., and Bassi, R. (1999) *J. Biol. Chem.* **274,** 33510–33521
24. Morosinotto, T., Castelletti, S., Breton, J., Bassi, R., and Croce, R. (2002) *J. Biol. Chem.* **277,** 36253–36261
25. Croce, R., Breton, J., and Bassi, R. (1996) *Biochemistry* **35,** 11142–11148
26. Caffarri, S., Croce, R., Cattivelli, L., and Bassi, R. (2004) *Biochemistry* **43,** 9467–9476
27. Moya, I., Silvestri, M., Vallon, O., Cinque, G., and Bassi, R. (2001) *Biochemistry* **40,** 12552–12561
28. Formaggio, E., Cinque, G., and Bassi, R. (2001) *J. Mol. Biol.* **314,** 1157–1166
29. Van Amerongen, H., and van Grondelle, R. (2001) *J. Phys. Chem. B* **105,** 604–617
30. Hayes, J. M., Gillie, J. K., Tang, D., and Small, G. J. (1988) *Biochim. Biophys. Acta* **932,** 287–305
31. Rogl, H., and Kuhlbrandt, W. (1999) *Biochemistry* **38,** 16214–16222